

Short term afterslip in the 1994 Sanriku-Haruka-Oki earthquake

Kosuke Heki and Yoshiaki Tamura

Division of Earth Rotation, National Astronomical Observatory, Mizusawa, Japan

Abstract. The Sanriku-Haruka-Oki earthquake, that occurred on December 28, 1994 at the Japan Trench as a typical interplate thrust event, was followed by year-long afterslip as large as the slip in the high-speed rupture [Heki *et al.*, 1997]. Here we report on the transition between these, inferred from crustal movements during the five days interval before and after the earthquake. Since this timescale is too long for seismometers but not suitably long for Global Positioning System (GPS), we rely primarily on strainmeter data taken ~200 km southwest of the epicenter. To confirm that the recorded strain changes are not local disturbances, we compare them with crustal movements derived by high time resolution analyses of GPS data in the same period. The transition to the long term afterslip was gradually achieved by slow fault slip with a time constant of a few hours. The cumulative slow slip in 24 hours amounts to ~1/3 of the coseismic slip, i.e. we may overestimate the coseismic displacement if we look at GPS data time series composed of daily solutions. The result presented here indicates that a single earthquake could have multiple aspects in its slowness, visible with different seismological and geodetic tools, and we need to use all such data to understand fully such a hybrid earthquake.

Introduction

Slip associated with modern and historic interplate earthquakes at the Japan Trench, off the Sanriku coast, Northeastern Japan accounts for only a portion of the time averaged rate of the Pacific plate subduction [e.g. Pacheco *et al.*, 1993; Kawasaki *et al.*, 1995]. This suggests that the deficit is taken up by slow processes, that are difficult to detect by conventional seismometric observations, including tsunami (slow) earthquakes, e.g. the 1896 Sanriku tsunami earthquake [Tanioka and Satake, 1996], ultra-slow earthquakes, e.g. the 1992 Sanriku ultra-slow earthquake [Kawasaki *et al.*, 1995]. Tsunami earthquakes have relatively long source times and excite tsunamis larger than expected from their surface wave magnitudes [Kanamori and Kikuchi, 1993]. The 1992 Ultra-slow earthquake had a source time as long as a day and did not excite even tsunami. Such earthquakes are perceptible only by geodetic means, e.g. strainmeters and tiltmeters [Kawasaki *et al.*, 1995]. The 1994 Sanriku-Haruka-Oki earthquake occurred at about midday (12:19:20.9UT) on 28/Dec/1994 at the Japan Trench (Fig. 1) as a typical interplate thrust event [Sato *et al.*, 1996; Tanioka *et al.*, 1996]. Records of permanent Global Positioning System (GPS) network showed that seismic moment comparable to the high-speed rupture was released over the one year postseismic period by afterslip [Heki

et al., 1997]. We refer to this as the “long term” afterslip. Here we study the transitional behavior from high-speed rupture to long term afterslip to clarify the existence of intervening slow fault movements with timescales shorter than a day.

To study the transitional fault movements, we require data with high stability and sensitivity for timescales as short as a few hours. In usual GPS data analyses, we estimate a set of site coordinates for a UT day observing session assuming the coordinates are stationary during the session. GPS has several technical problems although it has time resolution as high as its sampling intervals (typically 30 seconds). For example, multipath causes site-specific elevation dependent contamination of the phase data; it mainly affects vertical positions but may give rise to horizontal position errors when sky coverage of satellites is poor due to short observation times [Elósegui *et al.*, 1995]. In this study we focus on data from nearby extensometers whose performance is expected to be superior to that of GPS in this timescale. For comparison,

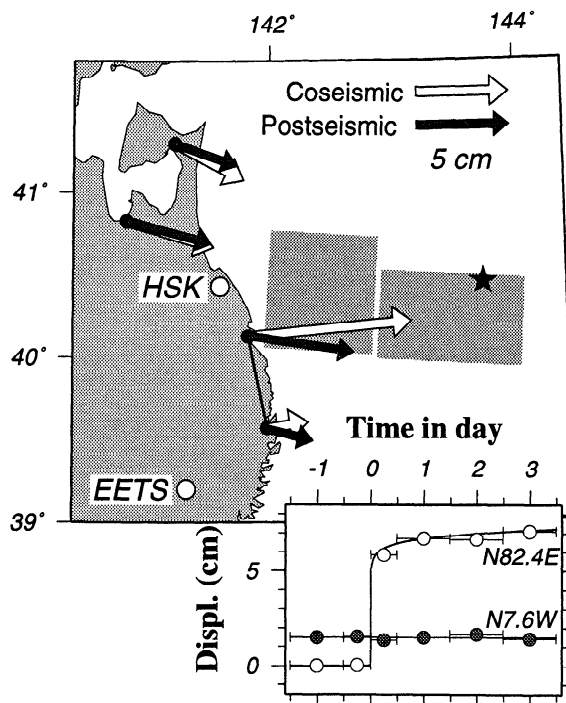


Figure 1. The epicenter of the mainshock of 28/Dec/1994 Sanriku-Haruka-Oki earthquake (star), four GPS stations (solid circles, Mutsu, Aomori, Kuji and Miyako from north to south), and two extensometers (open circles). The white and black arrows for GPS points denote their coseismic and 1 year cumulative postseismic movements with respect to Tsukuba [Heki *et al.*, 1997]. Fault planes of the long term afterslip are shown as dark gray rectangles. Inset shows Kuji-Miyako baseline vector changes for $t = -1.5 \sim 3.5$ (see caption of Figure 4).

Copyright 1997 by the American Geophysical Union.

Paper number 97GL03316.
0094-8534/97/97GL-03316\$05.00

we also analyze GPS data in the same period dividing the interval into shorter subsessions down to individual sampling epochs.

Extensometer Data

The 150 m long tunnel dug into a granite bedrock at the Esashi Earth Tides Station (EETS; 39.15N, 141.34E, Elevation 393 meters, Fig. 1) provides a stable environment for measurements of the Earth tides and continuous crustal deformation [Sato and Harrison, 1990]. We use crustal strain data at every 10 minutes interval measured with quartz tube extensometers in three directions, N-S, E-W and NE-SW. The response parameters for solid Earth tides and atmospheric pressure changes were estimated beforehand with data over a few months before and after the earthquake in order to isolate crustal strains related to the earthquake.

Figure 2a shows extension changes for $t = -1.5 \sim 3.5$ (t is the time in day after the earthquake). Four samples immediately after the earthquake (12:20~12:50UT) showed anomalous behaviors; the data are not low-pass filtered and might be affected by ground movement of the main- and aftershocks. Change before the earthquake ($t = -1.5 \sim 0.0$) is small, i.e., preseismic signals with timescales useful for short term earthquake prediction would not exceed a few % of the coseismic signals. The coseismic strain step (discontinuity at $t = 0$) is followed by postseismic strain change ($t = 0.0 \sim 3.5$) characterized by steep onsets and gradual decay. The asthenosphere is elastic for this timescale and the observed postseismic changes would indicate a slow phase of fault slip, similar to the one found by Kawasaki *et al.* [1995]. We refer to this as the "short term afterslip."

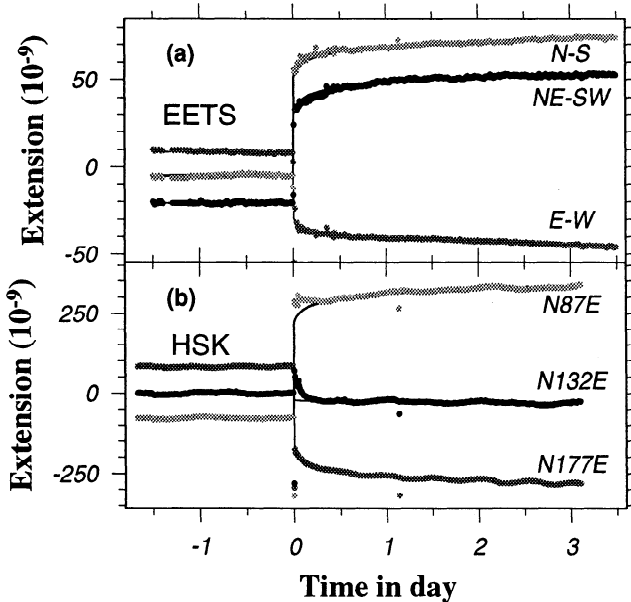


Figure 2. (a) Extension data taken with 10-minute interval in three directions, N-S (light gray), E-W (medium gray) and NE-SW (black), at the EETS for $t = -1.5 \sim 3.5$. Arbitrary biases are given in the vertical. Solid lines indicate the model; stationary for $t < 0$, discontinuity at $t = 0.0$, logarithmic decay (equation 1) for $t > 0$. (b) Extensometer data taken at HSK in the same period.

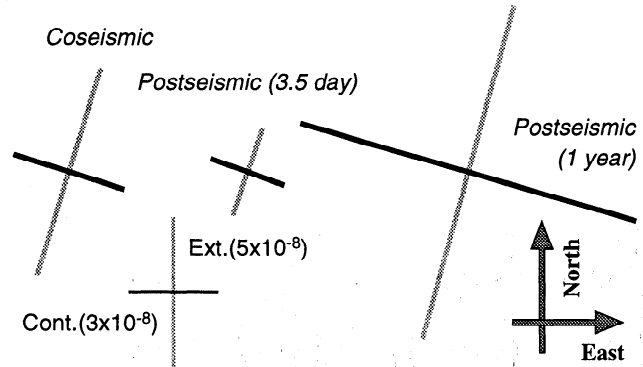


Figure 3. Diagram showing the principal axes of the strain changes at EETS caused by the earthquake. From left to right they are co-, short term (3.5 days) and long term (1 year) postseismic changes. The first two are observed at EETS, coseismic change as the difference between the last and the first valid readings before and after the earthquake, and short term postseismic change between 13:00UT 28/Dec/1994 and 24:00UT 31/Dec/1994. The last one is calculated assuming the long term afterslip fault parameters [Heki *et al.*, 1997] and an elastic half space.

Heki *et al.* [1997] suggested that the long term afterslip is differently distributed from the high-speed rupture, i.e., the former is evenly distributed over the fault surface while the latter concentrates in small asperities. Figure 3 compares principal axes of crustal strains at EETS for the three stages in which slip distribution differences should be reflected. The right one shows the 1 year strain change calculated assuming the parameters of the long term ($t = 0 \sim 365$) afterslip [Heki *et al.*, 1997] and an elastic half space. The left and middle ones show those observed at EETS for $t = -0.0 \sim +0.0$ and $t = +0.0 \sim 3.5$ respectively. These three are more or less similar, but the coseismic change has a larger NNE-SSW extension than its WNW-ESE contraction while they are comparable in the long term postseismic stage. The short term postseismic change is intermediate. Here we assume that the distribution of the short term afterslip in the fault plane is similar to that of the coseismic slip. This implies that the co- and short term postseismic changes are proportional for every component of every GPS point displacement as well as for every extension component. It much simplifies the treatments in the following sections.

The data in Figure 2a are fit to a model in order to infer the dispersion of the data and to provide a curve to fit the GPS data discussed later. Heki *et al.* [1997] modeled the long term afterslip with logarithmic decay $\alpha \ln(\beta t + 1)$, where α , β define overall amplitude and temporal decay respectively. We use the same formula for the short term changes but introduce a constraint of similarity between the short term afterslip and the coseismic slip. We express the extension in the i th direction ($i = 1, 2, 3$) $u_i(t)$ for positive t as

$$u_i(t) = p U_i + (1 - p) U_i \ln(\beta t + 1) / \ln(\beta + 1), \quad (1)$$

where U_i is the 1 day cumulative change composed of coseismic step $p U_i$ and postseismic changes $(1 - p) U_i$. The data $u_i(t)$ are measured relative to the pre-earthquake stationary levels, and four samples immediately after the earthquake are excluded. We estimated U_1 , U_2 , U_3 , p and β with iterative

nonlinear curve-fitting technique. The parameter β was estimated as $71.2 \pm 22.0 \text{ day}^{-1}$; a half of the cumulative change in 3.5 days is achieved in ~ 5 hours. Although this β is much larger than $6.5 \pm 0.6 \text{ year}^{-1}$ obtained for the long term afterslip [Heki *et al.* 1997], the observed changes are smooth throughout the period and the discrepancy may just indicate the limitation of applying a single formula for variety of timescales. The parameter p was estimated as 0.75 ± 0.02 , i.e. the strain changes in one day after the earthquake are composed of $\sim 3/4$ coseismic jump and $\sim 1/4$ slow postseismic change. The root-mean-square of the postfit residual was 0.8 nanostrain, i.e. the similarity constraint was reasonable at this level.

In Figure 2b we plot extensometer data from Hashikami (HSK, Fig.1) [Tohoku University, 1995] for comparison. It is a less sensitive (3 m long) extensometer, but is close to the epicenter and may provide additional information on the short term afterslip. The data are modeled with the same logarithmic decay using the same β and p as in EETS. The fit is fairly good for N177E component while discrepancies are seen during the first few hours after the earthquake for the other two components. There the quartz tubes are laid on Teflon bases, causing larger friction than in EETS (S. Miura, personal communication, 1997). Such discrepancies may indicate converging processes to static strain positions from mechanical imbalance caused by strong ground motions of the mainshock, rather than different fault slip distribution in the early postseismic stage visible only in near-fields.

GPS Data

Figure 1 shows "coseismic" (differences between 27/Dec/94 and 29/Dec/94) and cumulative postseismic movements in one year, of four GPS points closest to the epicenter [Heki *et al.*, 1997]. Here we reanalyze the Kuji-Miyako baseline (because of its large displacement signal and short length) using the Bernese GPS software version 3.4 [Rothacher *et al.*, 1993] to study the baseline vector changes in the same period as the strainmeter. Atmospheric delay was estimated in every 3-hour period. A modification was made to the original program GPSEST of the software so that site positions can be estimated for individual time intervals independent of those for atmospheric delays. IGS precise orbits and IERS Bulletin B earth orientation parameters were used.

The Figure 1 inset shows the changes of horizontal coordinate of Kuji with respect to Miyako. Each datum represents a conventionally defined UT day observing session, except 28/Dec/1994, for which the session was split into two $\sim 1/2$ day sessions at the earthquake occurrence time. To get maximum signal to noise ratio, horizontal coordinate changes are converted into those in N82.4E and N7.6W; directions parallel and perpendicular to the coseismic displacement of Kuji relative to Miyako. There is no significant displacement in N7.6W throughout the period while a slow postseismic movement is suggested in N82.4E. We modeled the latter with the logarithmic decay curve; the same p and β as EETS are assumed and the one day cumulative displacement (corresponding to U_i) is taken as the coordinate difference between 29/Dec/1994 ($t = 0.5 \sim 1.5$) and 27/Dec/1994 ($t = -1.5 \sim -0.5$).

In order to resolve short term postseismic movements, we divided each 24 hour session into four 6-hour subsessions

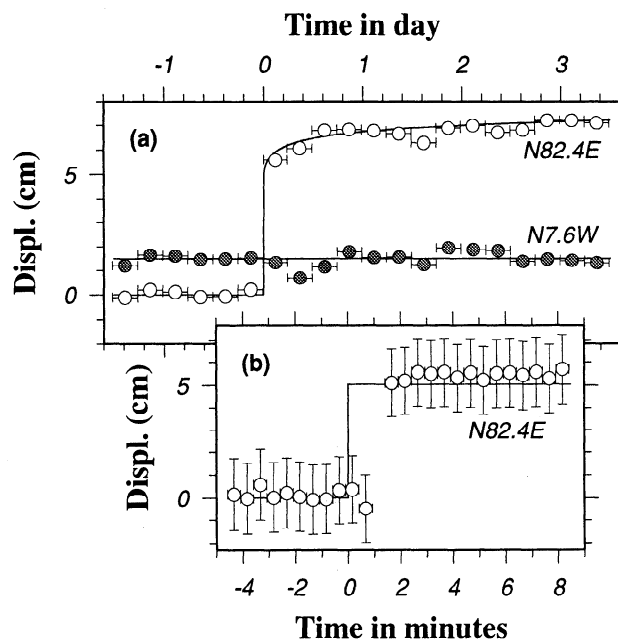


Figure 4. Horizontal movements of Kuji toward N82.4E (open circle) and N7.6W (solid circle, not plotted in (b)) with respect to Miyako. Horizontal axes show the time in day (a) and minute (b) after the earthquake. Arbitrary biases are given in the vertical axes. Thick black lines are model curves similar to Figure 2. Vertical errors indicate one sigma formal errors (smaller than symbols for (a)) and horizontal errors indicate periods represented by the data. Epoch-by-epoch solutions (b) have been corrected for multipath errors using the data one sidereal day earlier.

(sessions immediately before/after the earthquake are ~ 20 minutes longer/shorter than 6 hours because the earthquake did not occur exactly at 12:00UT) after resolving the phase ambiguities. Baseline solutions are increasingly sensitive to multipath as the occupation times decrease, but Genrich and Bock [1992] suggest they do not have to be modeled for site occupations longer than 1/2 hour. The results shown in Figure 4a are noisier than the extensometer data due possibly to multipath, but their overall trends are consistent with the model curve (the same curve as in Figure 1 inset). We may conclude that the slow postseismic change in the extensometer data represents real crustal strain related to the earthquake and not a local disturbance.

We finally try epoch-by-epoch coordinate solution for 12:15:00 \sim 12:27:30UT, 28/Dec/1994. Genrich and Bock [1992] showed that short period nondispersive multipath error could be filtered out by utilizing their daily repeatability. In Figure 4b daily signatures are removed by taking differences from the coordinate solutions one sidereal day earlier (i.e. 12:19:00 \sim 12:31:30UT, 27/Dec/1994). After the initial rupture start time (21:19:20.9UT), the coordinate remains stationary for more than 40 seconds (i.e. at two epochs 21:19:30 and 21:20:00UT), then it undergoes a large positive displacement (out of the vertical range of the figure) at 21:20:30UT and settles down at the new value at 21:21:00UT. Sato *et al.* [1995] suggested that the major seismic moment release started 26 seconds after the onset of the initial rupture. Then S wave would have taken another ~ 20 seconds to travel ~ 100 km (distance between Kuji and the location of the main

rupture); they in total would explain the observed delay of the coseismic jump. Again the data are consistent with the model "curve" (which is stretched in time and looks straight), that is, only 3/4 of the "coseismic" displacement (white arrows, Fig. 1) was really instantaneous.

Discussion

This study raises a question concerning the validity of joint inversion of tsunami and geodetic data to infer coseismic fault slip distribution [e.g. Tanioka *et al.*, 1996]. Tsunami data represent the fault movement with a timescale of a few minutes while regular GPS data analyses do not take account of motions within a day. They obviously could not be treated together to estimate a single fault parameter set for earthquakes with significant sub-day slip components.

Convergent plate interfaces are supposed to be composed of patches of unstable (velocity-weakening) field, stable (velocity-strengthening) field and compliant field [Pacheco *et al.*, 1993], and the 1994 earthquake is interpreted as a sequence with the high-speed rupture in the unstable field and the long term afterslip in the stable field with complementary distribution that equalizes the total slip throughout the fault plane [Heki *et al.*, 1997]. Crustal strain patterns at EETS (Fig. 3) may suggest that the short term afterslip occurred mainly in the compliant field that surrounds unstable patches.

The 1994 Sanriku-Haruka-Oki earthquake is the first interplate thrust earthquake whose fault slip has been documented in wide range of timescales from seconds to a year. An important lesson is that a single earthquake could have multiple aspects in its slowness, those of a normal earthquake, an ultra-slow earthquake and a year-long afterslip. It is an important issue if such a hybrid nature is common for other Sanriku earthquakes, such as the 1992 ultra-slow earthquake [Kawasaki *et al.*, 1995] and the 1896 tsunami earthquake [Tanioka and Satake, 1996]. Various tools, e.g. seismometers, tide gauges (to record tsunami), extensometers and space geodesy, allow us to see an earthquake through different time windows. We need to use all such devices if we are to understand fully a complex earthquake in a subduction zone.

Acknowledgments. We thank Tsuneya Tsubokawa, Sinzi Nakai for the EETS data, GSI staffs for RINEX GPS data, and Satoshi Miura

for providing the data from HSK. Critical reviews by Alan Linde significantly improved the quality of the paper.

References

- Elósegui, P., J. L. Davis, R. T. K. Jaldhag, J. M. Johansson, A. E. Niell, and I. I. Shapiro, Geodesy using the Global Positioning System: the effects of signal scattering on estimates of site position, *J. Geophys. Res.*, *100*, 9921-9934, 1995.
- Genrich, J. F., and Y. Bock, Rapid resolution of crustal motion at short ranges with the Global Positioning System, *J. Geophys. Res.*, *97*, 3261-3269, 1992.
- Heki, K., S. Miyazaki, and H. Tsuji, Silent fault slip following an interplate thrust earthquake at the Japan Trench, *Nature*, *386*, 595-598, 1997.
- Kanamori, H., and M. Kikuchi, The 1992 Nicaragua earthquake: a slow tsunami earthquake associated with subducted sediments, *Nature*, *361*, 714-716, 1993.
- Kawasaki, I., Y. Asai, Y. Tamura, T. Sagiya, N. Mikami, Y. Okada, M. Sakata, and M. Kasahara, The 1992 Sanriku-Oki, Japan, ultra-slow earthquake, *J. Phys. Earth*, *43*, 105-116, 1995.
- Pacheco, J. F., L. R. Sykes, and C. H. Scholz, Nature of seismic coupling along simple plate boundaries of the subduction type, *J. Geophys. Res.* *98*, 14,133-14,159, 1993.
- Rothacher, M., G. Beutler, W. Gurtner, E. Brockmann, and L. Mervart, Bernese GPS software version 3.4, Univ. of Bern, Switzerland, 1993.
- Sato, T., and J. C. Harrison, Local effects on tidal strain measurements at Esashi, Japan, *Geophys. J. Int.*, *102*, 513-526, 1990.
- Sato, T., K. Imanishi, and M. Kosuga, Three-stage rupture process of the 28 December 1994 Sanriku-oki earthquake, *Geophys. Res. Lett.*, *23*, 33-36, 1996.
- Tanioka, Y., and K. Satake, Fault parameters of the 1896 Sanriku tsunami earthquake estimated from tsunami numerical modeling, *Geophys. Res. Lett.*, *23*, 1549-1552, 1996.
- Tanioka, Y., L. Ruff, and K. Satake, The Sanriku-oki, Japan, earthquake of December 28, 1994 (M_w 7.7): rupture of a different asperity from a previous earthquake, *Geophys. Res. Lett.*, *23*, 1465-1468, 1996.
- Tohoku University, Faulting process of the 1994 Far East Off Sanriku earthquake inferred from GPS observation (in Japanese), *Rept. Coord. Committee Earthq. Pred.*, *54*, 97-101, 1995.

— K. Heki and Y. Tamura, Division of Earth Rotation, National Astronomical Observatory, 2-12 Hoshigaoka, Mizusawa, Iwate 023, Japan (email: heki@miz.nao.ac.jp; tamura@miz.nao.ac.jp)

(Received August 27, 1997; revised October 16, 1997; accepted November 4, 1997.)